P4.25 Improvement of cloud's spectral reflection simulation using MODIS cloud products

Seung-Hee Ham and Byung-Ju Sohn*
School of Earth and Environmental Sciences, Seoul National University, Seoul, South Korea

1. INTRODUCTION

Ice clouds are bright targets for the visible wavelength in the satellite measurement because these clouds reflect most of sunlight. Moreover, in the case of the moderate thick ice clouds which have large optical depth (greater than 10), most of lights are scattered before reaching lower troposphere, thus surface and atmospheric effects on satellite visible measurement can be minimized (Hu *et al,* 2004). Radiative transfer for ice cloud modeling needs only cloud optical properties rather than atmospheric and surface properties.

Cloud bidirectional reflectance distribution function (BRDF) can be calculated if accurate cloud products such as cloud optical thickness (COT) and effective radius are available. That is because, with reference satellite data especially cloud products, radiances at the satellite altitude can be simulated using Radiative Transfer Model (RTM). From this point of view, cloud BRDF simulation will be applicable for vicarious calibration for the satellite visible channel measurements using cloud targets.

In this study, radiative transfer modeling of ice clouds is developed and the accuracy of modeling is examined comparing calculated radiance with satellite measurement.

2. METHODOLOGY

2.1. *Radiative transfer modeling of ice clouds*

BRDF or normalized radiance leaving to the direction (μ, Φ) is defined as

$$BRDF = \frac{\pi I(\mu,\phi)}{F_0 \cos\theta} \tag{1}$$

where Φ is azimuth angle and μ is defined from zenith angle θ (μ = cosθ). Intensity I(μ, Φ) can be calculated using following Radiative Transfer Equation (RTE).

$$\mu \frac{dI(\tau,\mu,\phi)}{d\tau} = I(\tau,\mu,\phi) + \frac{\omega_0}{4\pi} F_0 P(\mu,\phi;-\mu_0,\phi) e^{-\tau/\mu_0} - \frac{\omega_0}{4\pi}\int_0^{2\pi}\int_{-1}^{1} I(\tau,\mu',\phi') P(\mu,\phi;\mu',\phi')\, d\mu' d\phi' \tag{2}$$

Because ω_0 is close to 1 for the cloud, BRDF is primarily a function of phase function P(μ, Φ; μ′, Φ′) and COT τ. This shows that angular distribution of BRDF can be determined by the angular distribution of phase function.

Santa Barbara Disort Atmohperic Radiative Transfer (SBDART) which can be used for calculation of cloud reflectance provides two types of cloud phase function.

First, Henyey-Greenstein (HG) phase function represented by asymmetry factor g is as follows.

$$p(\theta,g) = \frac{1-g^2}{(1+g^2-2g\cos\theta)^{3/2}} \tag{3}$$

Asymmetry factor can be parameterized by effective radius and the relationship varies with cloud phase. Community climate model 3 (CCM3) is used for the parameterization of single scattering albedo (ω) and extinction efficiency (Q_{ext}) as well as asymmetry factor (g) in terms of effective radius (R_e) as follows and the coefficients are mentioned in Table 1 (Ebert *et al*., 1992).

$$Q_{ext} = a + \frac{b}{R_e},\ 1-\omega = c + d \times R_e,\ g = e + f \times R_e \tag{4}$$

* Corresponding author: B. J. Sohn, School of Earth and Environmental Sciences, Seoul National University, Mail Code NS80, Seoul, 151-747, Korea
E-mail: sohn@snu.ac.kr

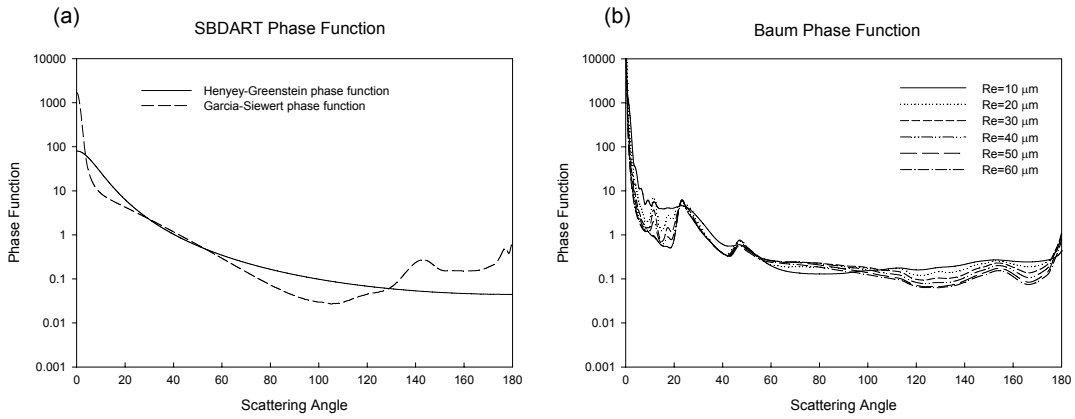

Fig. 1. (a) Two types of cloud phase function which are provided in SBDART (b) Ice cloud phase function of Baum which is based on *in-situ* measurements

Second, Garcia-Siewert (GS) phase function (Garcia *et al*., 1985) is calculated using Mie theory for water cloud particles. This assumption is not valid for ice cloud particles, however size distribution is based on *in-situ* measurements (Deirmendjian, 1964), GS function may provide reasonable accuracy. Cloud BRDF is less affected by cloud particle size for the case of GS function, because size distribution is fixed. In this study, including the Baum (Baum *et al*, 2005a and 2005b; Yang *et al.*, 2003a and 2003b) phase function (Figure 1), the impact of three types of phase function on the TOA radiance simulations is examined. Baum phase function is also based on reanalysis of *in-situ* data from a variety of midlatitude and tropical ice cloud field measurements. To get legendre coefficients of Baum phase function, the method of Hu *et al*. (2000) is used.

Bidirectional reflectance for MODIS geometry (μ, Φ) is calculated using RTM. MODIS cloud products such as COT and effective radius are used as inputs to the RTM.

2. 2. *Cloud pixel criteria*

MODIS cloud products are used not only for RTM inputs but also for selection of cloud pixels. Cloud top temperature (CTT) less than 205K, cloud top pressure (CTP) less than 213 hPa, and COT greater than 10

Table 1. Parametric coefficients in CCM3

	$\lambda < 0.69$	$0.69 < \lambda < 1.19$	$1.19 < \lambda < 2.38$	$2.38 < \lambda$
a	3.447×10^{-3}	3.448×10^{-3}	3.448×10^{-3}	3.448×10^{-3}
b	2.431	2.431	2.431	2.431
c	1×10^{-5}	1.1×10^{-5}	1.86×10^{-5}	0.46658
d	0	1.405×10^{-5}	8.328×10^{-4}	2.05×10^{-5}
e	0.7661	0.7730	0.794	0.9595
f	5.851×10^{-4}	5.665×10^{-4}	7.267×10^{-4}	1.076×10^{-4}

(λ: wavelength (μm))

are considered as ice clouds. In addition, to choose variations within surrounding 3x3 pixels less than 10 and 30 hPa respectively are used. To minimize directional effect of optical thickness, SZA and viewing angle are limited within 30°. Less than 0.05% of all pixels met this criteria. After carefully selecting horizontally homogeneous and optically thick cloud pixels, reflectances of cloud pixels are calculated.

3. DATA

Level 1B radiance and level 2 cloud product of MODIS data from January to December in 2004, are used. Equatorial ocean region centered in 125°E is investigated (Latitude 25°S~25°N, Longitude 95°E~155°E). All MODIS data are converted to 0.05° (~5 km) grid data and classified into clear and cloud pixels. For selected cloud pixels, satellite radiances are calculated using RTM and compared with MODIS measurements.

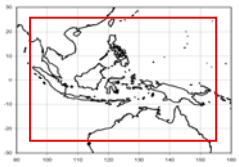

Fig. 2. Analysis domain (Latitude 25° S~25° N, Longitude 95° ~155° E)

4. RESULTS

4.1. *Cloud BRDF of three types of phase functions*

Cloud BRDF is calculated using SBDART for three cases of phase functions (HG, GS, and Baum functions). Figure 3 represents cloud BRDF for various phase functions and cloud particle effective radii when solar zenith angle (SZA) = 30 and COT=80. Each case shows different distribution from each other. For the case of HG function, strong reflection occurs in forward direction (Φ=0°) while reflection is dominant in backward direction (Φ=180°) for the cases of GS and Baum function as in King *et al* (1987). Such a maximum reflection occurs around viewing angle=30 for all cases. It shows that the specular reflection is dominant than diffuse reflection. In Figure 3 (b), cloud BRDF is almost constant with respect to particle size because phase function is fixed and only asymmetry factor is slightly affected by effective radius. Baum function is similar with GS function when effective radius is small (less than 20 μm) because size distribution which is used for calculation of GS phase function is from 0 to 20 μm.

4.2. *MODIS radiance simulation*

4.2.1. *MODIS geometry*

The Terra satellite carring the MODIS instrument is in sun synchronous orbit, thus the MODIS maintains almost constant viewing geometry throughout the year. Relative geometry changes are caused by annual variation of solar geometry. Figure 4 shows annual changes of relative geometry. Because geometry is not appeared around relative azimuth angle = ±90°, that is, MODIS data provides only limited satellite geometry.

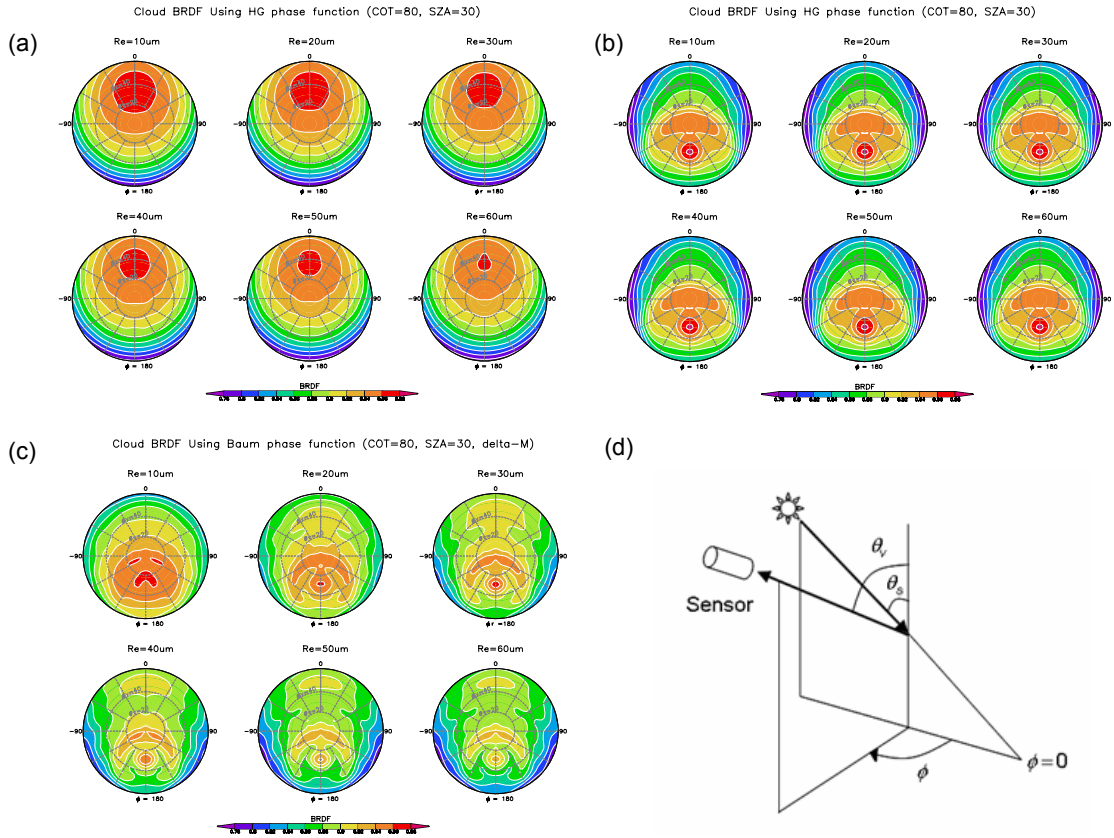

Fig. 3. Cloud BRDF for HG, GS, and Baum phase function. Radial axis and tangential axis mean sensor viewing angle and relative azimuth angle respectively. Relative azimuth angle=0 means forward propagating and it increases clockwise.

4.2.2. *Results of simulation*

Radiances are calculated using RTM for each geometry of cloud pixels and compared with measurements. Figure 5 shows scatter plots of measured and simulated radiances.

All three cases (HG, GS, Baum function) represent a linear relationship between observed and calculated values, however each has different bias and slope. The GS case represents the smallest bias while the HG function showed the largest bias and quadratic trend for high reflectance. However, we cannot conclude that GS function is the most realistic phase function because we did not examine various viewing geometry. In addition, we used MODIS cloud data which are adjusted values from observed radiance data; GS function may be the most similar phase function with the function used for the MODIS COT algorithm. We need a validation using other satellite data with various viewing geometry in order to determine the most appropriate cloud model and BRDF. Table 2 shows monthly variation of slope and intercept in Figure 5. GS function produces the slope slightly larger than 1, where HG function and Baum functions yield slopes smaller than 1. Intercept is the smallest when using GS function.

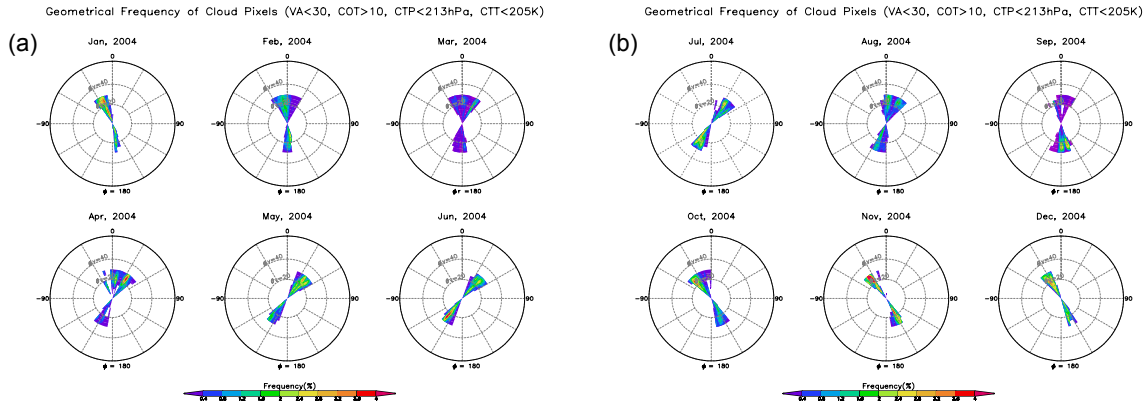

Fig. 4. Geometrical frequency of MODIS data in 2004: Sensor geometry is almost constant because satellite orbit is fixed locally in time. However, solar geometry varies throughout the year and it causes seasonal variation of relative geometry.

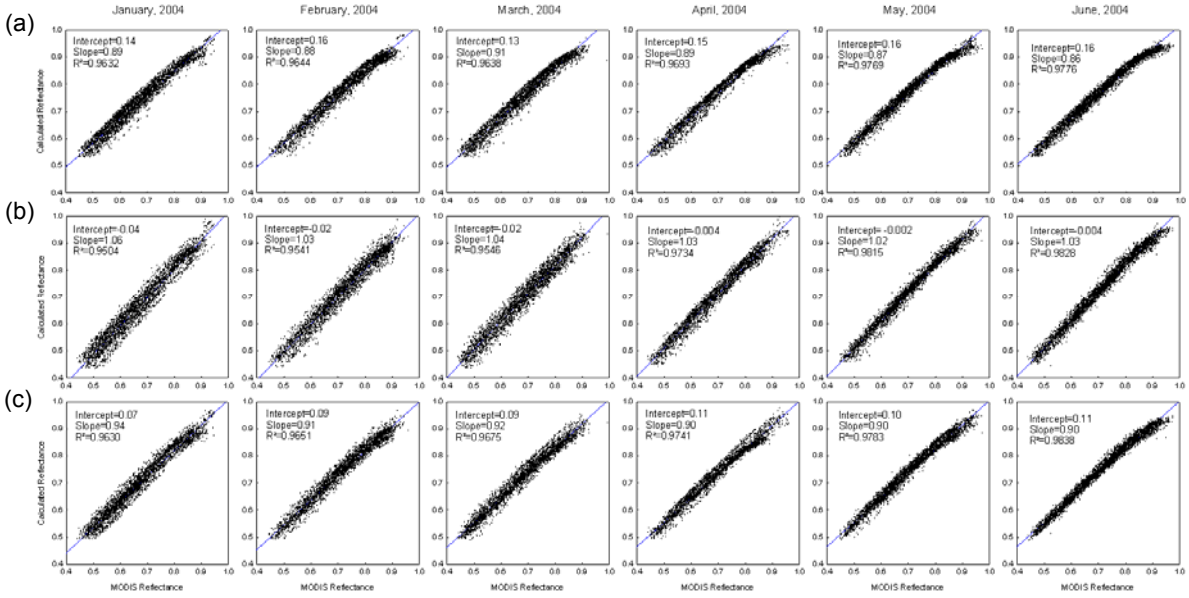

Fig. 5. Scatter plots of calculated and observed radiances for three phase functions from January to July in 2004. Each case represents different bias and slope while all three cases clearly show a linear relationship between two variables. (a) HG phase function (b) GS phase function (c) Baum phase function

Table 2. Slope and intercept of scatter plots in Figure 5.

		Jan	Feb	Mar	Apr	May	Jun	Jul	Aug	Sep	Oct	Nov	Dec
HG	Intercept	0.14	0.16	0.13	0.15	0.16	0.16	0.16	0.16	0.15	0.16	0.09	0.14
Funtion	Slope	0.89	0.88	0.91	0.89	0.87	0.86	0.85	0.87	0.86	0.85	0.91	0.88
GS	Intercept	0.04	−0.02	−0.02	0.004	−0.002	−0.004	0.02	0.001	0.01	−0.02	−0.02	0.03
Funtion	Slope	1.06	1.03	1.04	1.03	1.02	1.03	0.99	1.03	1.02	1.04	1.03	1.05
Baum	Intercept	0.07	0.09	0.09	0.11	0.1	0.11	0.1	0.09	0.09	0.09	0.1	0.08
Funtion	Slope	0.94	0.91	0.92	0.9	0.9	0.9	0.9	0.93	0.92	0.92	0.9	0.93

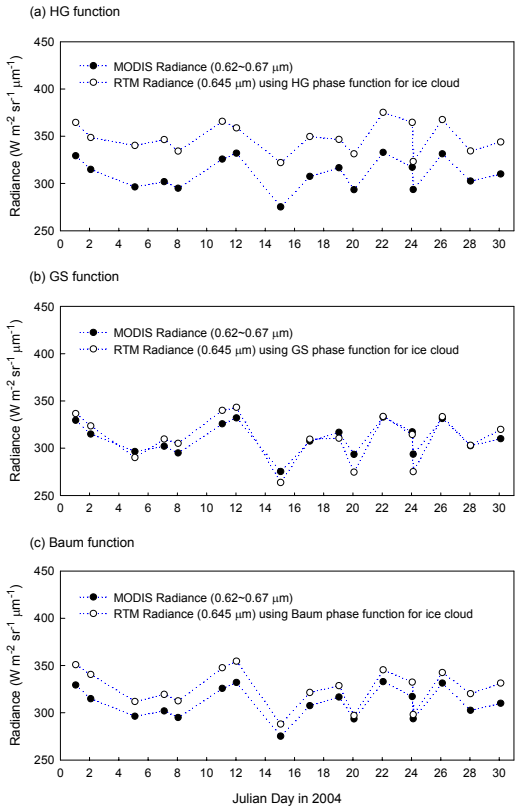

Fig. 6. Daily mean variations of calculated and observed radiances for three phase functions (January, 2004): Pixel values are averaged only if the number of cloud pixels at time are greater than 50.

Figure 6 shows time series of averages of calculated and observed radiances. For all three cases, simulated values represent similar trends (or gross features) with observed values, however each case shows different bias as shown in Figure 5. Because reflected flux value is a primarily function of COT, COT produces similar trends of all three case. However each phase function creates different angular distributions, this may gives different biases.

5. SUMMARY

Ice clouds reflect most of visible light, thus we need only cloud parameters rather than atmospheric and surface parameters to model cloud influence on TOA radiance. Using MODIS cloud products, ice cloud BRDF is calculated using three types of phase functions. Phase function is one of the important parameters affecting angular distribution of reflectance. Cloud BRDF using HG function represents a forward peak reflection, where as GS function and Baum function produce backward peak reflections. Although cloud surface is rough, a strong reflection occurs around viewing angle of 30° when SZA is 30°. It shows that specular reflection is dominant than diffuse reflection. Specific reflectance or normalized radiance is calculated using MODIS observation geometry for three types of phase functions and compared with observed values. It was noted that reflected fluxes are mainly a function of COT rather than a function of phase function. However, it was found that angular distribution of bidirectional reflectance or radiance is strongly affected by the phase function. Thus all three cases show a similar trend (large changes) but different biases (small changes). Nonetheless we cannot draw a conclusion that the phase function is the most realistic function from the results because MODIS observations do not provide various satellite geometries. We need more validation efforts using other satellite data from which various geometry effect can be examined.

Acknowledgments

The research was supported by the COMS Meteorological Program through a grant funded by KMA.

References

Baum, B. A., Heymsfield, A. J., Yang, P., and Bedka, S. T., 2005a: Bulk scattering models for the remote sensing of ice clouds. Part 1: Microphysical data and models. *J. Appl. Meteor*., 44, 1885-1895.

Baum, B. A., P. Yang, A. J. Heymsfield, S. Platnick, M. D. King, Y.-X. Hu, and S. T. Bedka, 2005b: Bulk scattering models for the remote sensing of ice clouds. Part 2: Narrowband models. *J. Appl. Meteor.*, 44, 1896-1911.

Deirmendjian, D., 1964: Scattering and polarization properties of water clouds and hazes in the visible and infrared. *Appl. Opt.,* 3, 187–196.

Ebert, E., and J. Curry, 1992: A parameterization of ice cloud optical properties for climate models. *J. Geophys. Res.,* 97, 3831–3836.

Hu, Yongxiang, Wielicki, B., Lin, B., Gibson, G., Tsay, S. C., Stamnes, K., and Wong, T., 2000: Delta-fit: A fast and accurate treatment of particle scattering phase functions with weighted singular-value decomposition least-square fitting, *J. Quant. Spectrosc. Radiat. Transf.*, 65, 681–690.

Hu, Yongxiang, Bruce A. Wielicki, Ping Yang, Paul W. Stackhouse Jr., Bing Lin, and David Young, 2004: Application of Deep Convective Cloud Albedo Observation to Satellite-based Study of Terrestrial Atmosphere: Monitoring Stability of Space-borne Measurements and Assessing Absorption Anomaly. *IEEE Transactions Geoscience and Remote Sensing,* vol 42, 11, 2594-2599.

King, M. D., 1987: Determination of the scaled optical thickness of clouds from reflected solar radiation measurements. *Journal of the Atmospheric Sciences*, 44, 1734-1751.

Garcia, R. D. M. and Siewert, C. E., 1985: Benchmark Results in Radiative Transfer, *Transport Theory and Statistical Physics*, 14, 437-483.

Yang, P., Yongxiang. Hu, D. M. Winker, J. Zhao, C. A. Hostetler, L. Poole, B. A. Baum, M. I. Mishchenko, and J. Reichardt, 2003a: Enhanced lidar backscattering by horizontally oriented ice crystal plates in cirrus clouds. *J. Quant. Spectros. Rad. Transfer,* 79-80*,* 1139-1157.

Yang, P., B. A. Baum, A. J. Heymsfield, Y.-X. Hu, H.-L. Huang, S.-C. Tsay, and S. A. Ackerman, 2003b: Single scattering properties of droxtals. *J. Quant. Spectros. Rad. Transfer,* 79-80*,* 1159-1169.